Development of High-Performance Solar Cells for the Jupiter and Saturn Environments

Andreea Boca[1], Jonathan Grandidier[1], Paul Stella[1], Philip Chiu[2], Xing-Quan Liu[2], James Ermer[2], Claiborne McPheeters[3], Christopher Kerestes[3], and Paul Sharps[3]

[1]Jet Propulsion Laboratory, California Institute of Technology, Pasadena CA 91109;
[2]Boeing Spectrolab Inc., Sylmar CA 91342; [3]SolAero Technologies Corp., Albuquerque NM 87123

***Abstract* — Many of the mission targets that NASA and the planetary-science community are interested in are located in deep space, in the 5-10AU range. This provides compelling motivation to develop solar cells and arrays that are highly efficient in low irradiance low temperature (LILT) environments. We give several examples of the iterative process our team has employed to develop cell designs that optimize the performance at LILT. We also provide results on advanced-architecture devices that have already demonstrated very high efficiencies in the Jupiter and Saturn LILT and radiation environments, specifically four-junction inverted metamorphic and triple-junction upright metamorphic solar cells, respectively.**

***Index Terms* — Jupiter, photovoltaic cells, Saturn, radiation hardening, space technology.**

I. Introduction

NASA and the planetary science community are interested in targets located far from the sun, such as in the Jupiter system (5-5.5AU), Jupiter-family and other comets, asteroid-belt and Trojan asteroids, the Saturn system (9.2-10AU) and beyond [1]. Even at such large sun distances, the power-source trades for mission concepts often favor solar arrays, primarily because of their reduced cost, ready availability, and good reliability. However, the high-AU environment is challenging for solar arrays: for example, at Jupiter the solar resource is only 3-4% of one sun and there is harsh charged-particle radiation; at Saturn the radiation is relatively mild but the irradiance is even lower, only 1% of one sun AM0 [2]. Consequently, solar arrays intended for 5-10AU mission concepts tend to be rather large, taking up a sizable fraction of system resources such as mass and stowed volume. Consider for example Europa Clipper, as the prototypical low-irradiance low-temperature (LILT) Flagship-class NASA mission, now in its planning stages [3]: the solar array mass takes up about a quarter of the whole spacecraft's dry mass of 2.5tons. This provides compelling motivation to develop smaller, more efficient LILT solar arrays, and the most leveraging knob to turn is at the device level. JPL has teamed up with Spectrolab and SolAero on several projects aimed at developing multijunction solar cells with high efficiency for the Jupiter and Saturn environments. This paper highlights some recent results to have emerged from these projects. Sections II and III give examples of the iterative process our team has employed to modify cell designs that had been originally developed for 1AU, in order to optimize their performance at LILT. Section IV provides results on advanced-architecture devices that have already demonstrated very high efficiencies in the Jupiter and Saturn LILT environments, specifically four-junction inverted metamorphic and triple-junction upright metamorphic solar cells, respectively.

II. LILT Optimization Example #1

The current state-of-practice (SoP) solar cell product for LILT is UTJ [4] from Spectrolab, powering the successful Juno spacecraft, launched in 2011, now in polar orbit around Jupiter. UTJ subscribes to a lattice-matched triple junction cell architecture, and it has demonstrated beginning-of-life (BOL) average efficiencies of ~28% under standard test conditions of 1AU +28°C, and ~30% under both Jupiter and Saturn conditions of 5.5AU -140°C and 9.5AU -165°C respectively [5]. Flight heritage makes UTJ a natural baseline design, as the starting point towards developing a LILT-optimized device.

As a first design iteration to depart from the baseline, we devised a modified version of UTJ which incorporates epitaxial design elements to increase the cell voltage. The performance of this 1st-iteration design was evaluated on eight bare cells of 3.98cm^2 active area each. All cells included in the sample set passed low irradiance room temperature (LIRT) screening per the criterion used in the Juno flight build, FF $\geq$ 0.77 at 5.5AU +28°C. A description of the LILT test laboratory setup can be found in [6]. Illuminated current-voltage (LIV) curves obtained on the 1st-iteration modified-UTJ are shown in Figure 1, with standard test conditions of 1AU +28°C in panel (a), and Jupiter LILT test conditions of 5.5AU -140°C in panel (b). The average and standard deviation efficiencies for the test sample set were 29.8% ± 0.2% at 1AU +28°C, and 29.7% ± 1.6% at 5.5AU -140°C, for an AM0 sun constant of 1367W/m^2. Although the 1AU performance shows clear improvement over the baseline, the LILT performance does not. As is obvious from Figure 1b, the disappointing LILT behavior is due to an unwanted reverse-biased junction characteristic near the solar cell's Voc, which reduces the fill factor. Note that the anomalous LIV curve shape is exclusively a LILT feature, not present in the 1AU +28°C data of Figure 1a.

We studied the photoactivity of the unwanted junction by testing the 1st-iteration modified-UTJ cells under variable light

intensity, while keeping the temperature constant at -140°C. The resulting data for an example cell is shown in Figure 2, with the full LIV sweeps in panel (a), and a zoom-in on the near-Voc region in panel (b). The other cells in the sample set showed the same qualitative behavior. The unwanted junction is photoactive, in that it acts as an additional solar cell, in series with the intended triple-junction cell, but with low photocurrent and poor reverse-breakdown voltage. Panel (c) shows the current at the shoulder of the LIV sweep, i.e. the max-power current or "Imp", for the unwanted junction, as a function of the short-circuit current or Isc for the full cell, the latter being proportional to the irradiance.

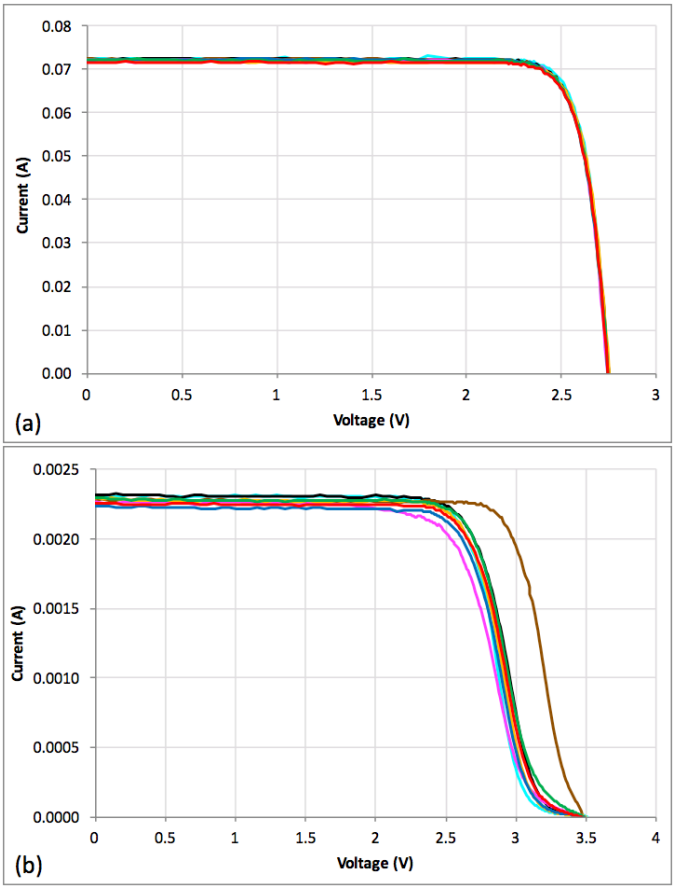

Figure 1. LIV sweeps on 1st-iteration modified-UTJ 3.98cm^2 solar cell samples at (a) 1AU +28°C; and (b) 5.5AU -140°C.

In a second design iteration, we devised a further-modified version of UTJ intended to eliminate the problem interface, while maintaining at LILT the performance advantage over baseline UTJ as demonstrated at 1AU. The performance of the 2nd-iteration modified-UTJ design was evaluated on nine bare cells of 27.22cm^2 active area each, pre-screened per the same LIRT criterion as the 1st-iteration sample set. LIV curves obtained on the 2nd-iteration cells are shown in Figure 3, with 1AU +28°C data in panel (a), and 5.5AU -140°C data in panel (b). Comparison with Figure 1 makes it clear that the fill-factor issue encountered at LILT for the first design iteration has been resolved by the second. The average and standard deviation efficiencies for the test sample set were 29.9% ± 0.2% at 1AU +28°C, and 35.2% ± 0.6% at 5.5AU -140°C. While the 1AU performance is virtually unchanged with respect to the 1st-iteration modified-UTJ, the LILT performance represents a marked improvement. More importantly, when compared to the baseline UTJ, the 2nd-iteration modified design is a drop-in replacement that provides ~17% more power at BOL, or equivalently that enables a ~17% smaller array size for a given power requirement.

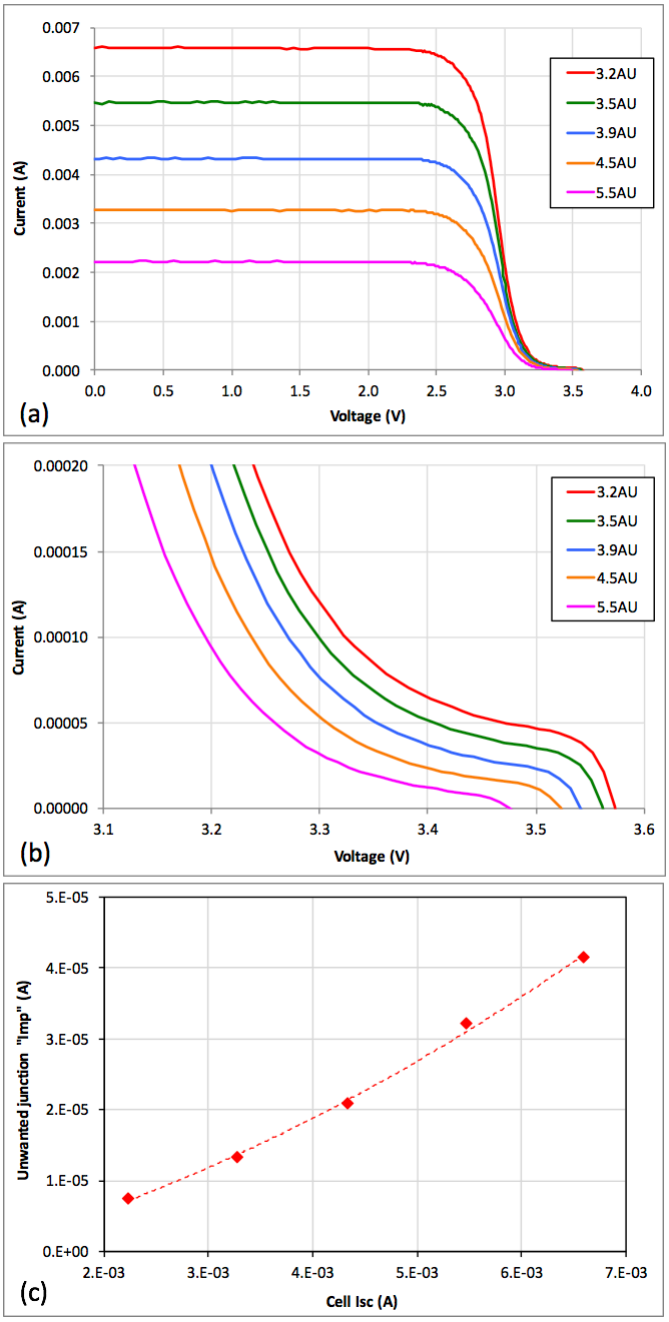

Figure 2. 1st-iteration modified-UTJ at -140°C and variable irradiance: (a) full fourth-quadrant LIV sweeps; (b) zoom in on near-Voc region; (c) current generated by the unwanted junction.

As a side note, this example illustrates that it is impossible to predict how well a cell will do at LILT based on data at standard test conditions. The 1st- and 2nd-iteration modified-UTJ have

nearly identical efficiencies at 1AU +28°C, but at LILT the latter produces almost 20% more power relative to the former.

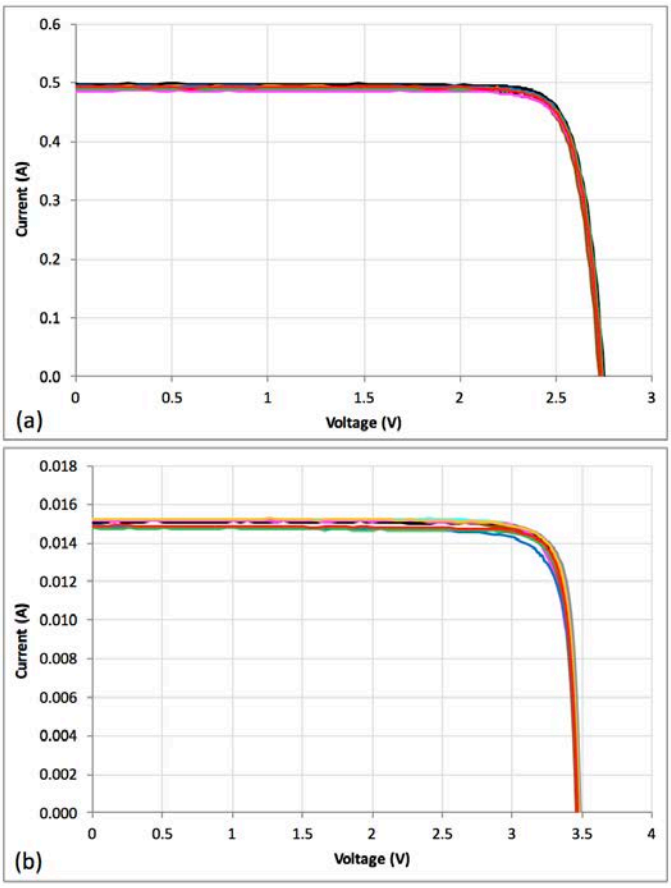

Figure 3. LIV sweeps on 2nd-iteration modified-UTJ 27.22cm^2 solar cell samples at (a) 1AU +28°C; and (b) 5.5AU -140°C.

On-going work on this cell type is evaluating the end of life (EOL) performance of modified-UTJ under Jupiter and Saturn conditions, and investigating avenues for further LILT performance improvement through additional design iterations.

III. LILT Optimization Example #2

As a second example, in this section we discuss modifying the design of inverted metamorphic quadruple junction (IMM4) solar cells, in order to optimize their performance under Saturn operating conditions of 9.5AU -165C.

IMM4 is an advanced architecture originally developed for 1AU applications. Compared to the lattice-matched triple-junction SoP, IMM4 has a bandgap combination that divides the AM0 spectrum more evenly among its subcells, leading to higher efficiency. This also makes it a promising candidate for high performance under LILT conditions.

We started out by evaluating the LILT performance of baseline, 1AU-optimized devices, as a first design iteration. Figure 4 shows the LIV curves for four IMM4 coverglassed interconnected cells (CICs) of active area 27.55cm^2 each, with standard test conditions of 1AU +28°C in panel (a), and Saturn LILT test conditions of 9.5AU -165°C in panel (b). These cells had all passed LIRT screening per the criterion FF ≥ 0.77 at 9.5AU +28°C. The average and standard deviation efficiencies for this sample set were 31.3% ± 0.4% at 1AU +28°C, and 32.3% ± 0.7% at 9.5AU -165°C. Of note in the LILT data is the sub-optimally low slope towards Voc (most pronounced for the red curve in Figure 4b), which limits the FF and hence the performance. If one were to only look at the fourth quadrant, one might erroneously conclude that the cause of this low slope is excessive series resistance. However, the curve shape in the first quadrant makes it clear that this device type actually contains an unwanted rectifying junction as well. Similar to the example in the previous section, the anomalous curve shape is not apparent in the 1AU data of Figure 4a, but rather is exclusively a LILT feature as shown in Figure 4b.

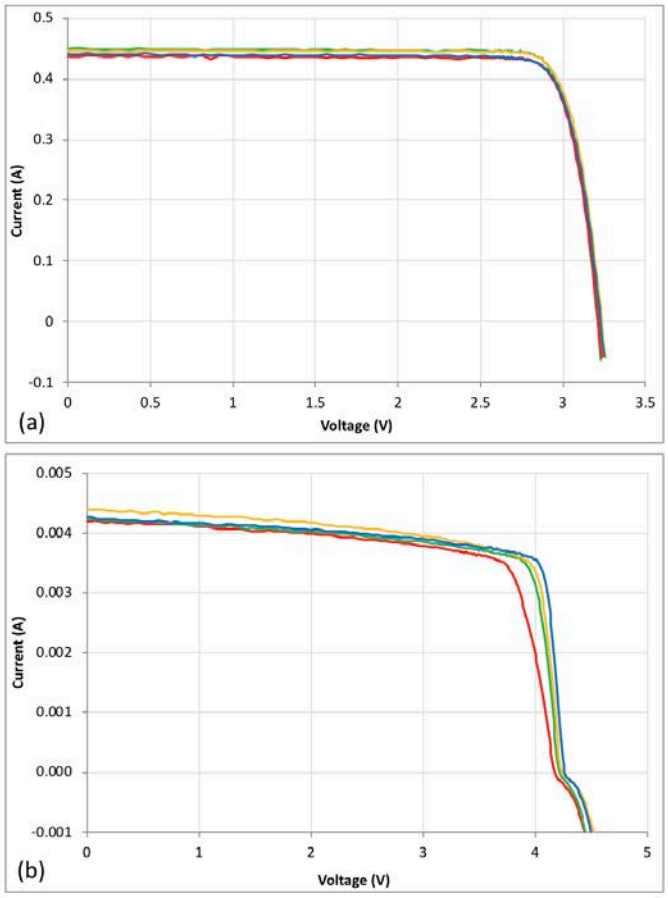

Figure 4. LIV sweeps on 1st-iteration baseline IMM4 27.55cm^2 CIC samples at (a) 1AU +28°C; and (b) 9.5AU -165°C.

To study the photoactivity of the unwanted junction, we tested the 1st-iteration IMM4 CICs under variable light intensity, while keeping the temperature constant at -165°C. The resulting data for an example cell is shown in Figure 5, with the full LIV sweeps in panel (a), and a zoom-in on the near-Voc region in panel (b). The other cells in the sample set showed the same behavior. In this case, the rectifying feature is not photoactive, suggesting that the problem interface is in a dark region of the cell.

As shown by Hoheisel et al. [7], LIV curve shapes such as those in Figure 5 can be caused by an unintentional majority carrier barrier formed at a passivation-interface layer intended to reflect minority carriers away from high surface

recombination regions, such as a back-surface field (BSF). Further clues to the location of the unwanted junction can be gleaned by looking at the low-temperature IV curve shapes of isotype (single active subcell) test structures.

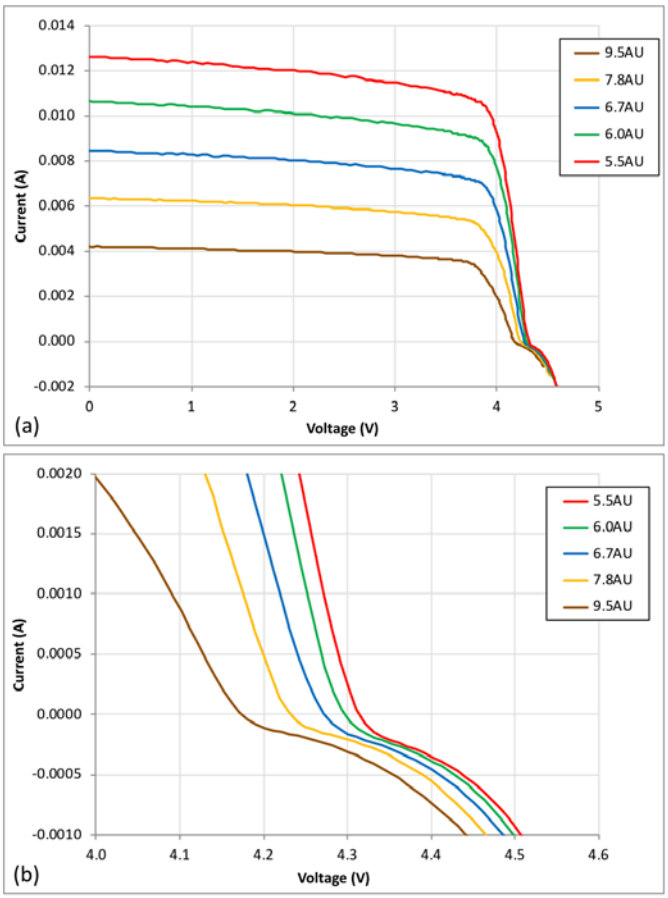

Figure 5. Baseline IMM4 at -165°C and variable irradiance: (a) full first and fourth-quadrant LIV sweeps; (b) zoom in on near-Voc region.

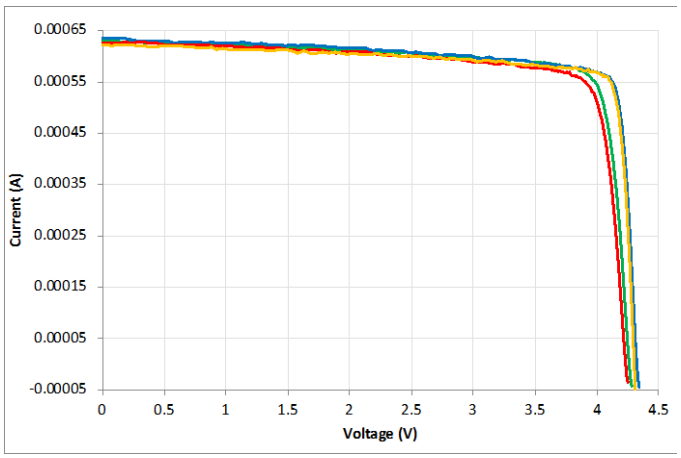

Figure 6. LIV sweeps on 2nd-iteration IMM4 4.02cm^2 bare cells at 9.5AU -165°C, showing improvement in the near-Voc region.

Based on considerations such as these, in a second design iteration, we devised a modified version of IMM4 intended to eliminate the problem interface.

Preliminary results on the modified-IMM4 design are shown in Figure 6. The tested devices were 4.02cm^2 bare cells and therefore not flight-representative in terms of absolute performance, however they were still useful for evaluating the qualitative curve shape relative to the baseline design. Note that the anomalous curve shape in the near-Voc region is nearly absent. The modified-design cells show 7% average improvement in P_{max} at 9.5AU -165°C, over baseline-design cells of the same configuration. Assuming that this performance delta can be maintained in flight-like large-area CIC devices, we estimate that the resulting Saturn-LILT average efficiency would be on the order of 35%. Demonstrating this improvement and incorporating further enhancements into the device design is work currently in progress.

IV. High-Efficiency Cells for Jupiter and Saturn

Solar cells most suitable for missions to the Jovian system require not only high BOL efficiency at LILT, but also the ability to withstand the harsh radiation environment with only minimal performance degradation. The Juno mission is unique for Jupiter, in that its orbit was specifically chosen to minimize the radiation dose; but for most other mission designs such as that being planned for Europa Clipper, the total dose is on the order of 3-5e15 1MeV e-/cm^2 (RDF = 2), and even significantly higher for long-lived lander or orbiter concepts. By contrast, for the Saturn system the radiation environment is relatively benign, with typical mission concepts having total-dose requirements on the order of only 2e14 1MeV e-/cm^2 (RDF = 2). On the other hand, the irradiance is a factor of ~3 lower than at Jupiter, which means that solar cells most suitable for Saturn missions are required to be particularly immune to LILT performance-limiting issues such as those covered in the previous two sections.

We will next highlight results on two advanced cell architectures now under development, that have shown very promising LILT performance. Specifically, an inverted metamorphic quadruple-junction (IMM4) design from SolAero has demonstrated high efficiency and remarkable radiation hardness under Jupiter test conditions [8]; and an upright metamorphic triple-junction (UMM3) design from Spectrolab has demonstrated high BOL efficiency under Saturn test conditions [6].

Figure 7 shows measured cell efficiencies as a function of temperature. Markers are averages over the respective test sample sets, the error bars are standard deviations, and the dashed curves are polynomial fits to aid the eye. Panel (a) shows IMM4 at a 5AU irradiance relevant to Jupiter, whereas panel (b) shows UMM3 at a 9.5AU irradiance relevant to Saturn. All samples were CICs, LIRT-screened per a FF $\geq$ 0.77 criterion at +28°C BOL, IMM4 at 5AU and UMM3 at 9.5AU. The sample quantity was 6 each at BOL and EOL for IMM4, and 5 at BOL for UMM3. In the case of IMM4, the EOL radiation dose was 4e15 1MeV e-/cm^2; prior to irradiation of the EOL population, we ensured that it had the same LILT average efficiency as the BOL population, to within <0.1% absolute.

For IMM4, the efficiency at 5AU -125°C was 37.9% ± 1.2% at BOL, and 29.5% ± 1.0% at EOL. This represents a significant

performance improvement over the SoP at both BOL and EOL. In particular, we note that the LILT power remaining fraction P/P0 = 0.78 after 4e15 1MeV e-/cm^2 is significantly higher than the P/P0= 0.68-0.72 that one would expect based on SoP cells under standard test conditions. For UMM3, the efficiency at 9.5AU -165°C BOL was 35.4% ± 1.2%, which is a performance improvement over all SoP-architecture cells that we have evaluated under Saturn conditions [5].

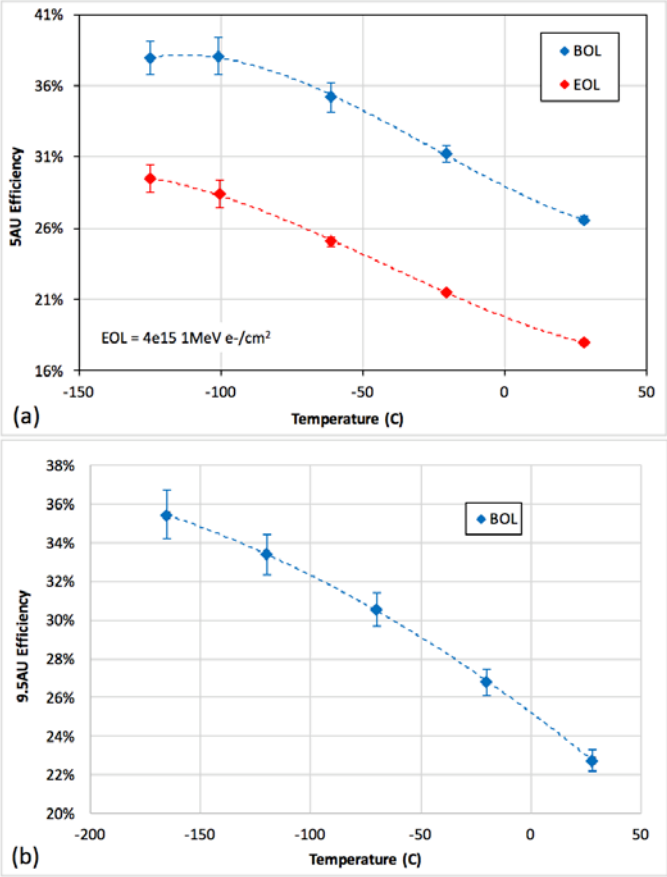

Figure 7. CIC efficiency as a function of temperature for (a) IMM4 under Jupiter irradiance; and (b) UMM3 under Saturn irradiance.

V. Conclusions

We have provided examples of the performance-limiting issues that are unique to the LILT operation environment, and of how such issues can be ameliorated through appropriate modifications to the solar cell design.

We showed that the IMM4 architecture is highly suitable for the Jupiter-system environment, having demonstrated BOL and EOL average efficiencies on the order of 38% and 30%, respectively. We also showed that the UMM3 architecture is highly promising for the Saturn-system environment, with demonstrated average BOL efficiencies in excess of 35%. Applying the LILT design optimization process on these advanced architectures is expected to yield further performance improvements in the near term.

VI. Acknowledgement

The authors thank Molly Shelton, Karen De Zetter, Bob Kowalczyk and Clara MacFarland of JPL for taking the LIV data shown in this paper; and Fred Elliott and Jeremiah McNatt of NASA GRC for management of the EESP project for the STMD/GCD program.

This research was carried out at the Jet Propulsion Laboratory, California Institute of Technology, under contract with the National Aeronautics and Space Administration.

References

[1] "Visions and voyages for planetary science in the decade 2013-2022", National Research Council, 2011; "NASA selects two missions to explore the early solar system" and "NASA invests in concept development for missions to comet, Saturn moon Titan", retrieved from www.nasa.gov/press-release on 1/12/2018.

[2] W. Atwell, "Radiation environments for deep-space missions and exposure estimates", AIAA SPACE, 2007.

[3] A. Ulloa-Severino et al., "Power subsystem approach for the Europa mission", 11th ESPC, 2016.

[4] "Ultra triple junction (UTJ) 28.3% solar cells", retrieved from www.spectrolab.com/datasheets/cells on 1/12/2018.

[5] P. Stella et al., "LILT testing of solar cells for the Juno mission", 21st SPRAT, 2009; A. Boca et al., "A data-driven evaluation of the viability of solar arrays at Saturn", IEEE JPV 7, 2017.

[6] A. Boca et al., "Advanced-architecture high-efficiency solar cells for LILT applications", 44th IEEE PVSC, 2017.

[7] R. Hoheisel et al., "Experimental analysis of majority carrier transport processes at heterointerfaces in photovoltaic devices, IEEE JPV 2, 2012; and "Low temperature effects in photovoltaic devices for deep space missions", 42nd IEEE PVSC, 2015.

[8] A. Boca et al., "Solar arrays for LILT and high-radiation environments", retrieved from ntrs.nasa.gov on 1/12/2017.